# Zirconium-based isoreticular metal-organic frameworks for CO$_2$ fixation via cyclic carbonate synthesis

**Hye-Min Jeong, Roshith Roshan, Robin Babu, Hyeon-Jun Kim, and Dae-Won Park[†]**

Division of Chemical and Biomolecular Engineering, Pusan National University, Busan 46241, Korea

**Abstract**−Two highly stable isoreticular metal-organic frameworks comprising chains of zirconium coordinated with linkers of 1,4-H$_2$BDC (1,4-benzenedicarboxylic acid) and 4,4′-H$_2$BPDC (4,4′-biphenyldicarboxylic acid), denoted as MIL-140A and MIL-140C, were synthesized. The catalytic activity of these frameworks was studied for the coupling reaction of CO$_2$ and epoxides to produce cyclic carbonates under solvent-free conditions. Excellent activity was observed for both catalysts: they yielded high epoxide conversion with >99% selectivity toward the cyclic carbonate, and were fully reusable even after four cycles without any considerable loss of initial activity. The enhancement in the catalytic activity was explained based on acidity/basicity studies. The influence of various reaction parameters such as catalyst amount, reaction time, reaction temperature, and CO$_2$ pressure was also investigated. Reaction mechanism was proposed on the basis of experimental evidence and our previous DFT (density functional theory) studies.

Keywords: MIL-140A, MIL-140C, Carbon Dioxide, Epoxide, Cyclic Carbonate

## INTRODUCTION

Our planet is on the edge of global warming intimidations, and hence, it is high time that we take the necessary steps to regain a balance over the carbon cycle. With carbon dioxide (CO$_2$) being the main greenhouse gas resulting from human activities, its capture and sequestration are imperative. Several technologies are being proposed for the capture and sequestration of CO$_2$ [1-7]. However, the high thermodynamic stability of CO$_2$ makes its permanent fixation a cumbersome task. Hence, the conversion of CO$_2$ into value-added products is highly relevant. Cyclic carbonate products are widely employed as solvents in Li ion batteries, paints, and grease, and for pharmaceutical and polymer products [8,9]. Although the cycloaddition of CO$_2$ with highly reactive epoxides to form cyclic carbonates is thermodynamically feasible, the reaction rates are often negligible owing to the high stability of CO$_2$ molecules. To overcome this, several catalysts have been developed, of which a Lewis acidic metal center in association with a halide ion co-catalyst nucleophile represents the most typical binary system [10-14].

Metal organic frameworks (MOFs), which are well-known organic-inorganic hybrid materials, have been found to be highly efficient in materializing the epoxide-CO$_2$ transformation in the presence of nucleophilic co-catalysts. High selectivity toward the desired products was achieved, in addition to appreciable yields at ambient temperatures, which are highly desirable for energy conservation. The extra edge of MOF/co-catalyst systems over common metal oxide/co-catalyst systems is attributed to the high porosity of MOFs, which endows them with better CO$_2$ adsorption ability and even distribution of catalytic active sites [15-18].

Although the syntheses of several Zr-based MOFs have been reported in the last decade, they were sparsely employed for catalytic studies, and even more rarely for effectuating CO$_2$ conversion, with the exception of UiO-66. UiO-66 was found to be catalytically active in the CO$_2$ conversion process [19-22]. Because of the high oxidation state of Zr, the Zr-based MOFs show high possibility for activating the epoxide substrates and good stability (reusability). However, in some cases UiO-66 required the presence of an organic solvent such as chlorobenzene [22]. We determined that an investigation into the catalytic efficiency of a thermally stable Zr-MOF under relatively mild reaction conditions without the use of solvent for CO$_2$-epoxide cycloaddition could enrich the library of heterogeneous catalysts available for this important organic transformation. Two zirconium oxide based MIL metal organic frameworks (MIL-140A and MIL-140C) were first synthesized by Guillern et al. [23] in 2012, and reported to have high hydrothermal and a good mechanical stability. We selected these MOF for their catalytic application in the cycloaddition of CO$_2$ and epoxides for the first time. The frameworks comprise chains of zirconium coordinated with linkers of 1,4-H$_2$BDC (1,4-benzenedicarboxylic acid), and 4,4′-H$_2$BPDC (4,4′-biphenyldicarboxylic acid), respectively. The materials differ in their pore size (3.2 and 5.7 Å) and surface area (415 and 670 m$^2$g$^{-1}$) [24,25]. The catalytic activities observed for these MOFs were explained on the basis of various experimental and physicochemical characterization results.

## EXPERIMENTAL

### 1. Preparation of Catalysts

MIL-140A was prepared according to a previously reported method [25]. 40 mmol (6.7 g) of 1,4-benzenedicarboxylic acid (BDC; Aldrich, 98%) and 20 mmol (4.7 g) of ZrCl$_4$ (Aldrich, 99.9%) were

[†]To whom correspondence should be addressed.
E-mail: dwpark@pusan.ac.kr

introduced into a Teflon-lined steel autoclave and 1,621 mmol (125 mL) of DMF was added. The mixture was stirred for a few minutes at room temperature and then at 220 °C. After 16 h of heating, the autoclave was cooled slowly, followed by centrifugation and washing with DMF. Thereafter, the material was soaked in methanol for 12 h to remove the DMF from the pores. This was repeated three times, and the material was dried in vacuum at room temperature.

MIL-140C was synthesized in a similar manner as MIL-140A. 10 mmol (2.42 g) of biphenyl-4,4′-dicarboxylic acid (4,4′BPDC; Aldrich, 97%) and 5 mmol (1.17 g) of $ZrCl_4$ (Aldrich, 99.9%) were introduced into a Teflon-lined steel autoclave. 25 mmol (1.43 mL) of acetic acid and 324 mmol (25 mL) of DMF were added, and the mixture was stirred for a few minutes at room temperature and then heated at 220 °C for 12 h.

## 2. Characterization of Catalysts

Powder X-ray diffraction (XRD) patterns were recorded with PANalyticalX'pert PRO power diffractometer using Ni-filtered Cu Kα radiation ($\lambda$=1.5404 Å, time per step=4 s). Fourier transform infrared (FT-IR) spectra were obtained on an AVATAR 370 Thermo Nicolet spectrophotometer with a resolution of 4 cm$^{-1}$. Thermogravimetric analysis (TGA) was conducted on a Netzsch ST 449 instrument. The surface morphology involved using an S-4200 field emission scanning electron microscope (FE-SEM, Hitachi-3500 N). The elemental analysis (EA) was performed with a Vario ELIII system. The metal content was obtained from ICP-OES analysis using ULTIMA2CHR (1.5 kW, 40.68 MHz, 130-800 mm) with mono chromato HDD and a poly chromato PMT detector. $CO_2$ and $NH_3$ TPD profiles were acquired with a chemisorption analyzer (BEL-CAT).

## 3. Cycloaddition of $CO_2$ and PO

Propylene carbonate was synthesized from PO and $CO_2$ in a 25 mL stainless-steel autoclave equipped with a magnetic stirrer. For each typical semi-batch operation, PO (18.6 mmol) and the MIL-140 catalyst (and co-catalyst, wherever applicable) were introduced into the reactor without solvent, and the reactor was pressurized with $CO_2$ at room temperature. The reactor was heated to the desired temperature, and the reaction was started by stirring at 600 rpm by maintaining the reactor pressure constant with a back-pressure regulator. When a desired reaction time had elapsed, the reaction was stopped and the reactor was cooled externally to 0 °C using an ice bath. The mixture was centrifuged to separate the catalyst, and the liquid products were analyzed with a gas chromatograph (GC, Agilent HP 6890 A) equipped with a capillary column (HP-5, 30 m×0.25 μm) using a flame ionization detector. Toluene was used as the internal standard.

## RESULTS AND DISCUSSION

## 1. Characterization of Catalysts

The powder XRD pattern of the synthesized MIL-140A and MIL-140C catalysts was similar to that of the literature reported (Fig. 1). The FT-IR spectra of MIL-140A and MIL-140C are shown in Fig. 2. The C=O bond stretching at 1,700 cm$^{-1}$, characteristic of the free BPCD linker, shifts to 1,620 cm$^{-1}$ in the spectrum of MIL-140C, and a Zr-O bond peak at 500 cm$^{-1}$ appears, confirming the
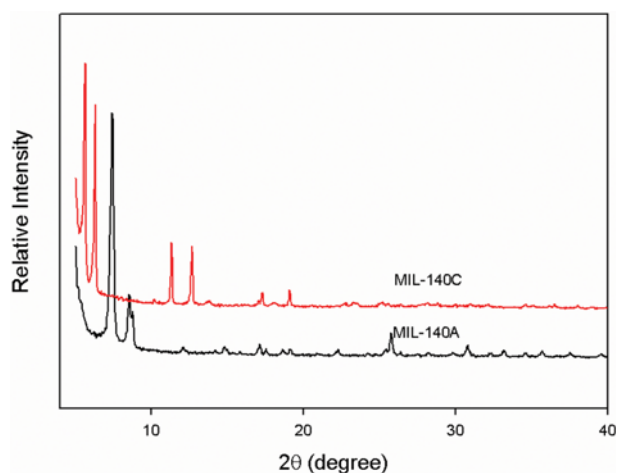


Fig. 1. X-ray diffraction patterns of synthesized MIL-140A and MIL-140C.
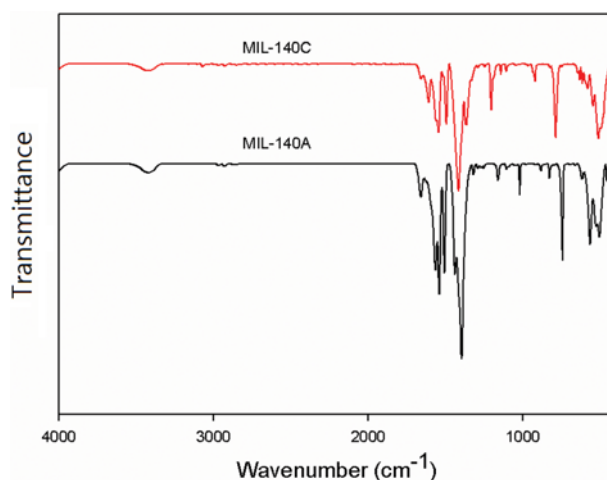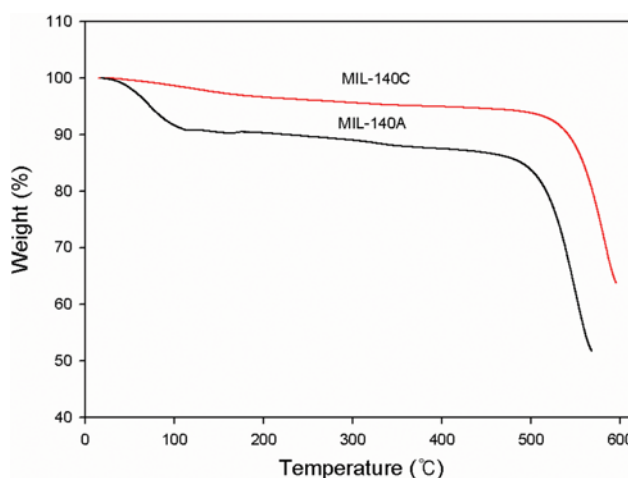


Fig. 2. FT-IR analysis of MIL-140A and MIL-140C.



Fig. 3. TGA analysis of MIL-140A and MIL-140C.

formation of the MOF.

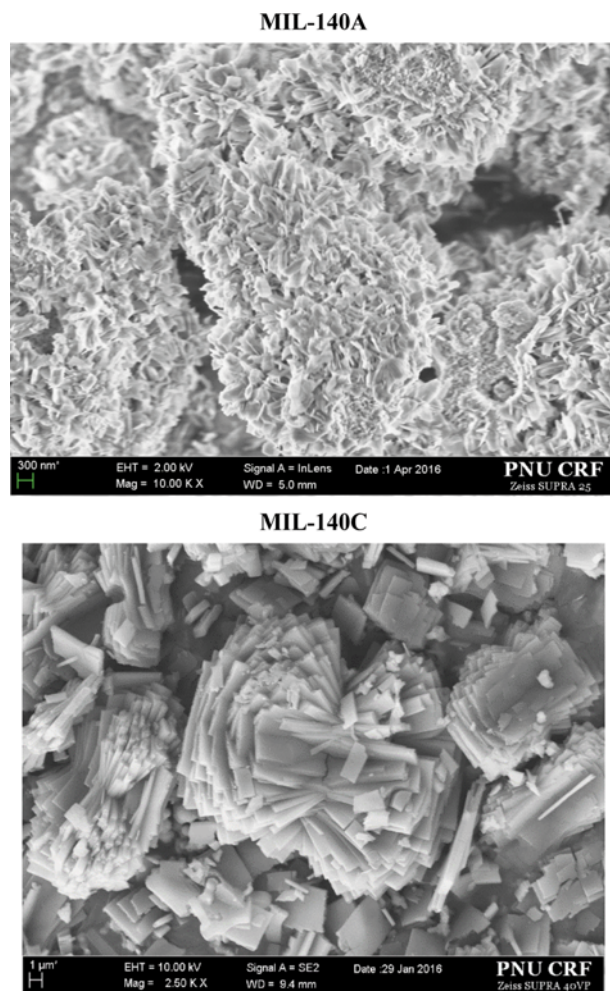The TGA data shown in Fig. 3 indicate the high thermal stabil-

**MIL-140A**



**MIL-140C**



Fig. 4. FE-SEM image of MIL140 A and MIL-140C.

ity of the framework formed. No severe degradation occurred before 520 °C (5 wt%), which is well above the reaction temperatures of the cycloaddition tests studied here, making MIL-140A and MIL-140C very stable catalysts. The FE-SEM images of the MIL-140A and MIL-140C materials (Fig. 4) also revealed their morphology.

Elemental analysis of the synthesized MIL-140A gave the results C, 35.32; H, 2.52; O, 27.94 wt%; these are similar to the calculated values of C, 35.4; H, 1.47; O, 29.5. ICP-OES showed the Zr content in MIL-140A to be 32.14 wt%. Elemental analysis of the synthesized MIL-140C gave the results C, 48.83; H, 2.51; O, 21.97 wt%, which were consistent with the calculated values of C, 48.4; H, 2.32; O, 22.52. ICP-OES revealed the Zr content in MIL-140C to be 24.44 wt%. The surface area calculated for MIL-140A from the $N_2$ adsorption isotherms at 77 K was 403 $m^2$/g, whereas the surface area of MIL-140C was estimated to be 814 $m^2$/g. The $N_2$ adsorption and desorption curves for both the samples are given in the supporting information (Fig. S1, Fig. S2). The pore size of MIL-140A and MIL-140C was 3.2 and 5.7 Å, respectively.

## 2. Cycloaddition of $CO_2$ with Epoxides

Propylene oxide (PO) was used as the substrate to evaluate the catalytic activity of MIL-140A and MIL-140C. As shown in Table 1, at 80 °C and 1.2 MPa $CO_2$ pressure, no significant conversion of

Table 1. Catalytic tests of MIL-140A and MIL-140C in the cycloaddition of PO and $CO_2$

| Entry | Catalyst | Conversion (%) | Selectivity (%) |
|---|---|---|---|
| 1 | None | 0 | - |
| 2 | ZrCl$_4$/BDC/TBAB | 20 | 95 |
| 3 | ZrCl$_4$/BPDC/TBAB | 20 | 93 |
| 4 | MIL-140A | 0 | - |
| 5 | MIL-140C | 0 | - |
| 6 | TBAB | 15 | 98 |
| 7 | TBAI | 20 | 97 |
| 8 | MIL-140A/TBAB | 82 | >99 |
| 9 | MIL-140C/TBAB | 79 | >99 |
| 10 | MIL140A/TBAI | 19 | >99 |
| 11 | MIL-140C/TBAI | 10 | >99 |

Reaction conditions: PO=42.8 mmol, $CO_2$ pressure=1.2 MPa, cat.=0.2 mol%, temperature=80 °C, time=6 h, semi-batch

PO occurred with both MIL-140A and MIL-140C alone in 6 h (Table 1, Entries 4, 5). However, in the presence of a common co-catalyst such as tetrabutyl ammonium bromide (TBAB), there was a drastic increase in the PO conversion (to 79-82%), along with high propylene carbonate selectivity (>99%) (Table 1, Entries 8, 9) for both catalysts. Since TBAB is a known homogeneous catalyst for $CO_2$-epoxide cycloaddition, its standalone activity was also tested as a control experiment. However, under the employed reaction conditions (80 °C, 1.2 MPa $CO_2$, 6 h), the conversion of PO with TBAB alone was significantly lower (Table 1, Entry 6) compared with that observed using MIL-140A/TBAB and MIL-140C/TBAB binary systems, indicating the synergistic catalysis operated via the Lewis acid centers of MIL-140A/MIL-140C and the nucleophilic anion of the co-catalyst. To ascertain the role of the MOF environment in the catalysis, another set of control experiments were conducted with the precursors of MIL-140A and MIL-140C. The conversion of PO was lower in comparison to those yielded by the MIL-140/TBAB systems, thus affirming the highly favorable nature of the MOF environment for the catalysis (Table 1, Entries 2, 3). The even distribution of the active centers and the $CO_2$ adsorption capabilities of the MOF network must have been the driving forces for the effective catalysis.

MIL-140C exhibited a higher BET surface area and pore size compared with MIL-140A. Hence, higher catalytic activity was expected for MIL-140C, but the catalytic activity of MIL-140A was only marginally higher than that of MIL-140C. To find the reason behind the difference in catalytic activity, $CO_2$- and $NH_3$-temperature programmed desorption (TPD) analyses were performed on both catalysts to examine the acid-base characteristics. The total adsorbed $CO_2$ for MIL-140A was obtained as 17 mmol g$^{-1}$, which is the amount of basic sites in the catalyst (Fig. S3). Similarly, in the case of $NH_3$-TPD, the number of acidic sites was equivalent to 0.24 mmol g$^{-1}$, which corresponded to the metal centers (Fig. S4). In the case of MIL-140C, $CO_2$-TPD was found to be around 15 mmol g$^{-1}$ and $NH_3$-TPD was estimated around 0.21 mmol g$^{-1}$ (Figs. S5, S6). Thus, it is evident that in a broader view, the acidity/basicity of the MOF plays an important role in $CO_2$-epoxide cyc-
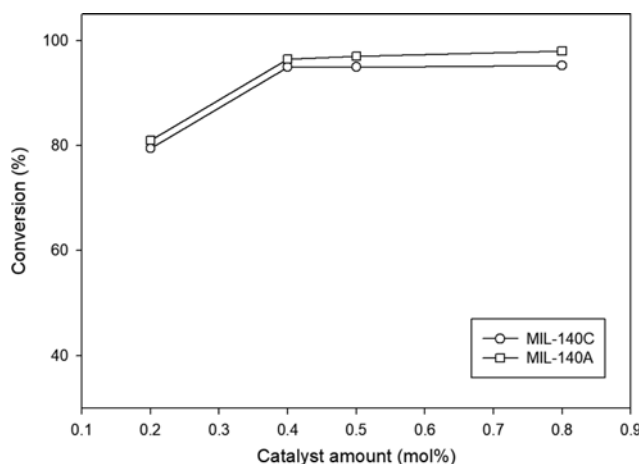
**Fig. 5. Effect of catalyst amount on the reactivity of MIL-140A and MIL-140C (Reaction conditions: PO=42.8 mmol, cat.=MIL-140A and C, co-cat.=TBAB (0.2 mol%), temperature=80 °C, time=6 h, $CO_2$ pressure=1.2 MPa).**



**Fig. 7. Effect of $CO_2$ pressure on the reactivity of MIL-140A and MIL-140C (Reaction conditions: PO=42.8 mmol, cat.=MIL-140 (0.2 mol%), co-cat.=TBAB (0.2 mol%), temperature= 80 °C, time=6 h).**

loaddition reactions. Metallic Lewis acid site is known to activate epoxide oxygen, and basic site accelerates $CO_2$ activation [26-30].

The various reaction parameters for the MIL-140A and MIL-140C catalysts were optimized as follows. The effect of catalyst amount was examined in the range 0.2-0.8 mol% (each) with 42.8 mmol of PO at 80 °C, 1.2 MPa $CO_2$ for 6 h (Fig. 5). A stable increase in the PC yield was noticed from 0.2 (82%) to 0.5 mol% (96%) for the MIL-104A/TBAB catalyst system, with a maximum conversion of 97% at 0.8 mol%. The result shows that even with a four-fold increase in the catalyst amount (mol%), the increment in PC yield was only 15%. An almost similar order of activity was observed for the MIL-104C/TBAB catalyst system. This leads to the observation that small amounts of MIL-140C/TBAB and MIL-140C/TBAB systems are sufficient to achieve moderate to good yields of PC with excellent selectivity. Hence, 0.2 mol% of the binary systems was used to further optimize the other reaction conditions.

Similarly, the temperature dependence of MIL-140/TBAB in effectuating the $CO_2$-PO cycloaddition was investigated. For MIL-140A/TBAB, the catalytic activity increased from 40 °C to 100 °C, with the PO conversion reaching its maximum PO conversion of 93% at 100 °C for 6 h at 1.2 MPa of $CO_2$ pressure (Fig. 6). A similar trend was observed for the MIL-140C/TBAB, whereby a PO conversion of 92% was achieved for 6 h at 1.2 MPa.

The effect of $CO_2$ pressure (0.3 to 3.0 MPa) on the PO conversion for both catalysts is displayed in Fig. 7. For the MIL-140A/TBAB system, the PO conversion increased steadily from 56% to 96% with a pressure increase from 0.3 to 1.5 MPa, which clearly indicates the dependence of the catalytic activity on the concentration of available $CO_2$ at the reactive sites. However, very high $CO_2$ pressures proved detrimental to the efficiency of the MIL-140A/TBAB catalyst system, as the PO conversion decreased steeply from 95% to 75% in the range of 1.5 to 3 MPa. This decrease in PO
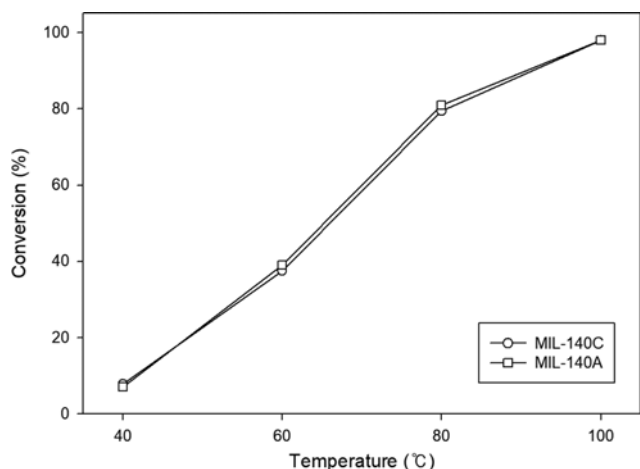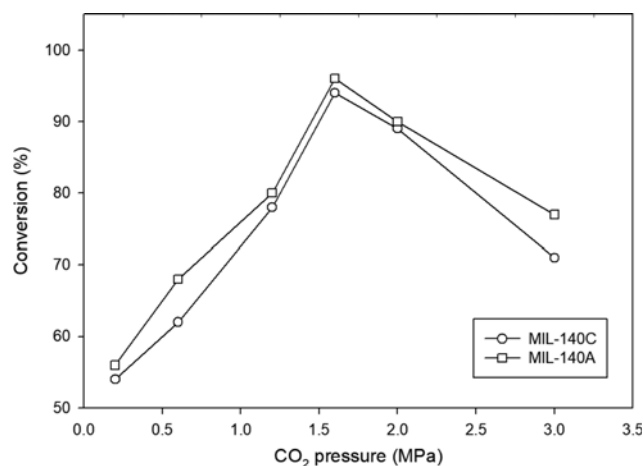


**Fig. 6. Effect of temperature on the reactivity of MIL-140A and MIL-140C (Reaction conditions: PO=42.8 mmol, cat.=MIL-140 (0.2 mol%), co-cat.=TBAB (0.2 mol%), time=6 h, $CO_2$ pressure=1.2 MPa).**
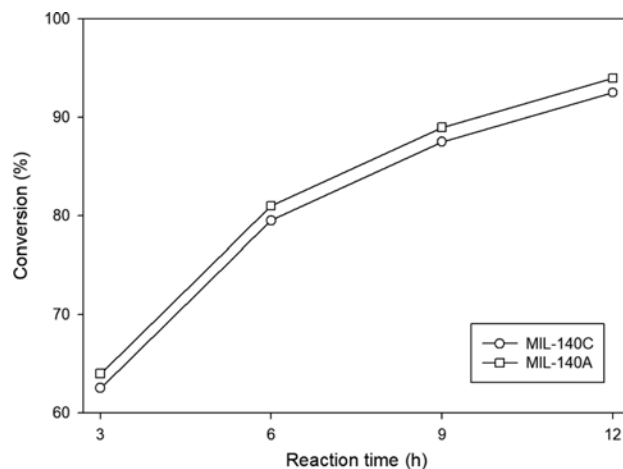


**Fig. 8. Effect of reaction time on the reactivity of MIL-140A and MIL-140C (Reaction conditions: PO=42.8 mmol, cat.=MIL-140 (0.2 mol%), co-cat.=TBAB (0.2 mol%), temperature= 80 °C, $CO_2$ pressure=1.2 MPa).**

**Table 2. Performance of MIL-140A and MIL-140C for the synthesis of various cyclic carbonates**

| Epoxide | Catalyst | Conversion (%) | Selectivity (%) |
|---|---|---|---|
| Propylene oxide | MIL-140A | 82 | >99 |
| Epichlorohydrin | MIL-140A | 80 | >99 |
| Styrene oxide | MIL-140A | 73 | 98 |
| Cyclohexene oxide | MIL-140A | 9 | 93 |
| Allylglycidyl ether | MIL-140A | 85 | 97 |
| Propylene oxide | MIL-140C | 79 | >99 |
| Epichlorohydrin | MIL-140C | 78 | >99 |
| Styrene oxide | MIL-140C | 69 | 97 |
| Cyclohexene oxide | MIL-140C | 7 | 93 |
| Allylglycidyl ether | MIL-140C | 84 | 97 |

Reaction conditions: Epoxide=42.8 mmol, cat.=MIL-140 (0.2 mol%), co-cat.=TBAB (0.2 mol%), temperature=80 $^\circ$C, time=6 h, $CO_2$ pressure=1.2 MPa, semi-batch

conversion is analogous to many porous catalyst systems wherein the dilution effect of excess $CO_2$ near the reactive sites inhibits efficient interaction of the substrate with the catalyst. A similar trend was also observed for the MIL-140C/TBAB catalyst system, where the PC increased steadily from 55% to 92% when the pressure was increased from 0.3 to 1.5 MPa. The effect of reaction duration on the MIL-140A/TBAB and MIL-140C/TBAB binary catalyst-mediated cycloaddition of PO and $CO_2$ is shown in Fig. 8. The PO con-

version increased from 3 h to 12 h, and the highest conversion was obtained at 12 h.

To check the versatility of the MIL-140/TBAB catalyst system, various epoxides were also subjected to $CO_2$ cycloaddition under identical reaction conditions (Table 2). Terminal epoxides such as allylglycidyl ether, PO, and epichlorohydrin were converted in excellent to moderate yields. However, cyclohexene oxide showed very low conversion probably due to the steric hindrance of the epoxide, as is commonly observed with most of the metal-organic framework catalyst systems [31-33].

The mechanism for the Zr-based catalyst in PC synthesis is proposed based on the experimental results and our previous DFT studies [34-37]. As shown in Scheme 1, initially the O atom of the PO interacts with the Lewis acid center (Zr atom) of the catalyst to form a Zr-O bond, which weakens the PO ring. Subsequently, ring opening occurs and the bromide ion from the TBAB co-catalyst attacks the $\beta$ carbon atom of the PO. This leads to the formation of an alkoxy halide intermediate, which in turn reacts with the $CO_2$ to form a carbonate complex. The halide ion leaves the circuit and cycloaddition commences to afford the desired PC along with the regeneration of the catalyst. The observation that TBAB works much better than TBAI with the MIL-140C catalyst (Table 1, Entries 9, 11) leads to the conclusion that the catalysis primarily occurs in the inner channels or pores of the MOF. Since iodide is a larger anion compared to bromide, it has less accessibility to the reactive centers, as reported in a few other cases too [38-41].

The reusability performance of a catalyst system is an import-
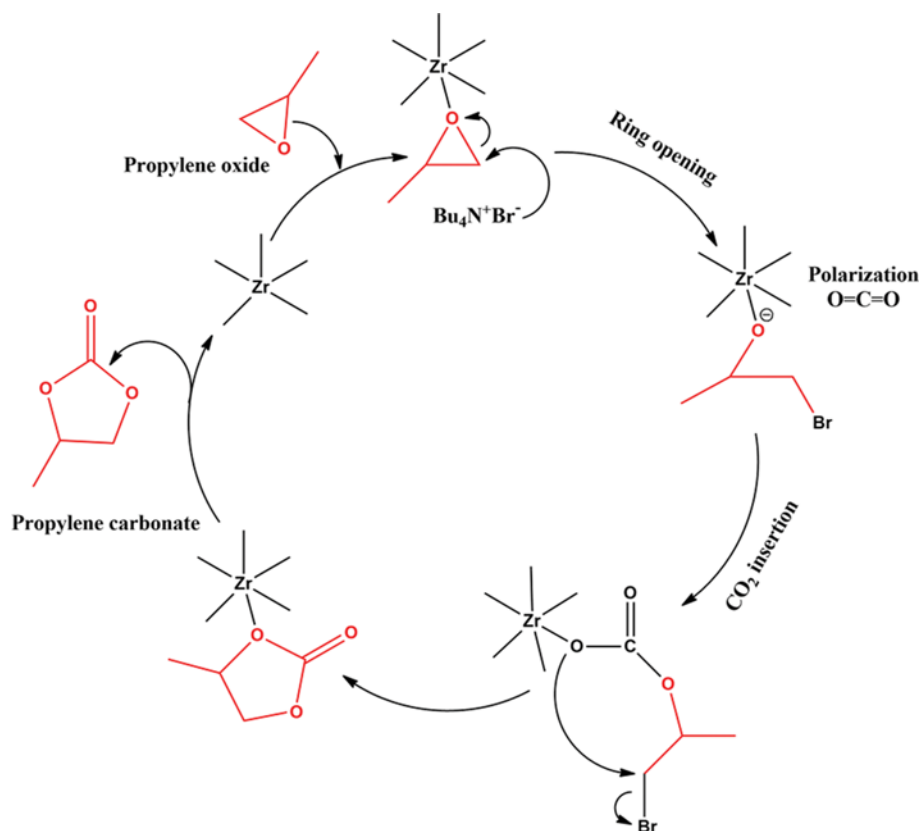


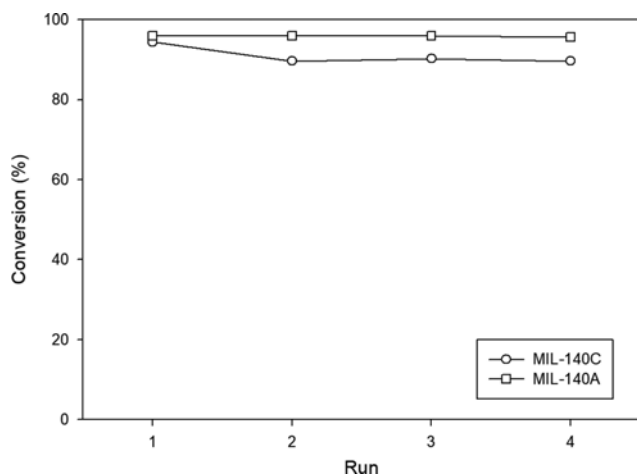Scheme 1. Reaction mechanism containing the role of MIL-140 catalyst.

**Fig. 9. Reusability performance of MIL-140A and MIL-140C (Reaction conditions: PO=42.8 mmol, cat.=MIL-140 (0.4 mol%), co-cat.=TBAB (0.4 mol%), temperature=80 °C, time=6 h, $CO_2$ pressure=1.2 MPa).**
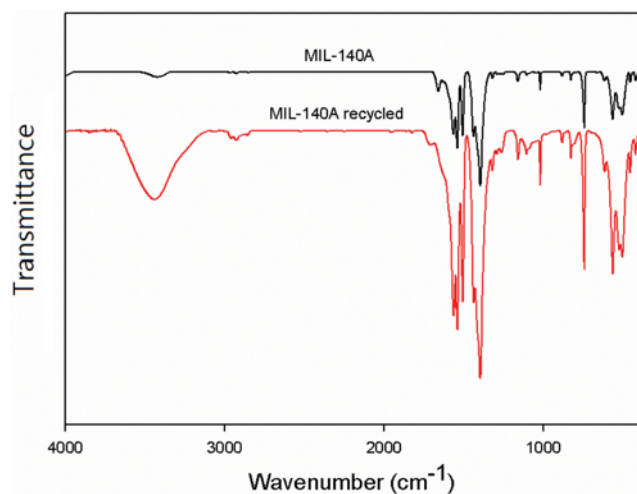


**Fig. 10. FT-IR analysis of synthesized and recycled MIL-140A.**
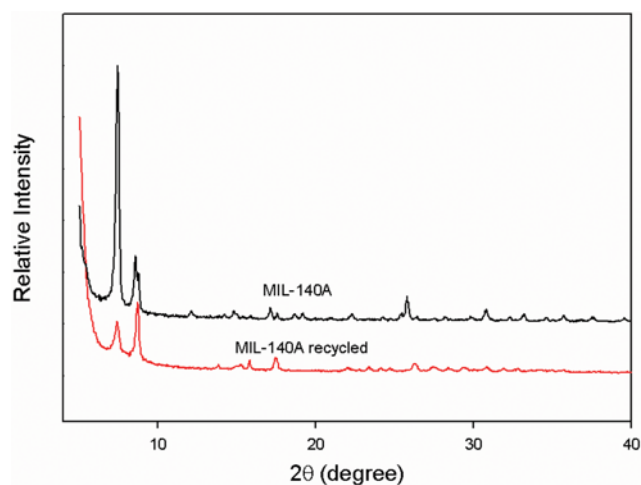


**Fig. 11. X-ray diffraction patterns of synthesized and recycled MIL-140A.**
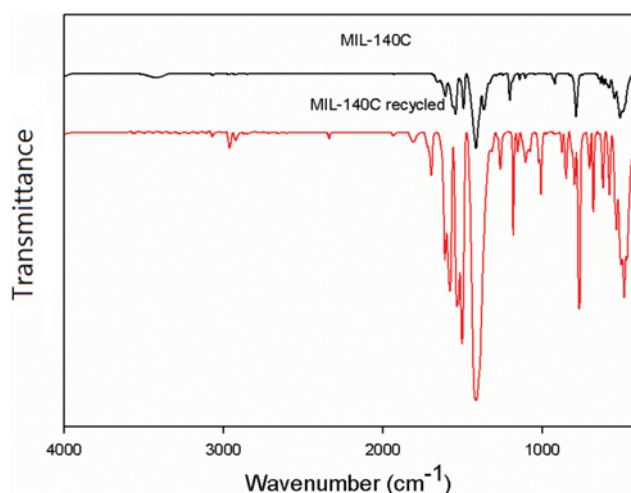


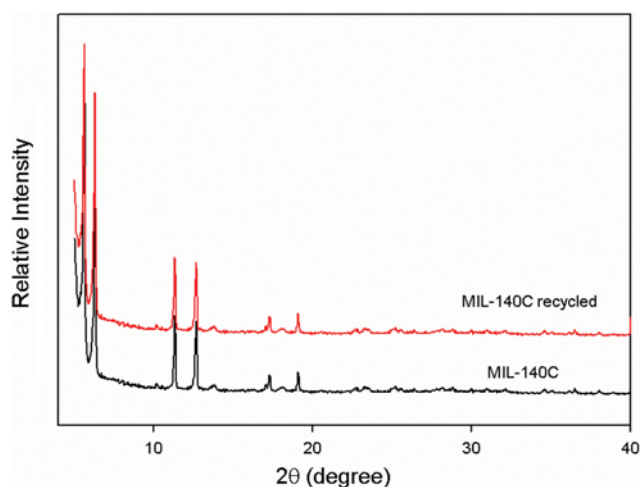**Fig. 12. FT-IR analysis of synthesized and recycled MIL-140C.**



**Fig. 13. X-ray diffraction patterns of synthesized and recycled MIL-140C.**

ant criterion to be analyzed critically to ensure its stability and efficiency. Thus, we analyzed the reusability of both MIL-140A/TBAB and MIL-140C/TBAB systems under the optimized conditions (Fig. 9). Near-complete reusability was exhibited by both catalysts, and the conversion (PO) and selectivity (PC) remained almost similar to that of the freshly used catalyst even after four cycles. The PXRD and FT-IR peaks after four cycles were similar to those for the freshly prepared catalysts (Fig. 10-13). This clearly proves the chemical stability of MIL-140A and MIL-140C for use as heterogeneous catalysts in $CO_2$ insertion reactions even with highly substrates such as epoxides.

## CONCLUSIONS

Two highly stable zirconium based metal-organic frameworks consisting of zirconium coordinated with linkers of 1,4-$H_2$BDC (1,4-benzenedicarboxylic acid) (MIL-140A) and 4,4'-$H_2$BPDC (4,4'-biphenyldicarboxylic acid) (MIL-140C) were synthesized and characterized using various physico-analytical techniques. High catalytic

activity was obtained for both MIL-140A and MIL-140C under mild reaction conditions, with high selectivity for propylene carbonate (>99%) in the cycloaddition of propylene oxide and $CO_2$ with TBAB as the co-catalyst. The high catalytic activity was explained based on acidity/basicity studies. Recyclability tests indicated no significant change in the catalytic activity up to four cycles, and the heterogeneity of the catalyst was confirmed by using PXRD and FT-IR analyses. A plausible mechanism was suggested based on experimental inferences and our previous DFT studies.

## ACKNOWLEDGEMENTS

## SUPPORTING INFORMATION

Additional information as noted in the text. This information is available via the Internet at http://www.springer.com/chemistry/journal/11814.

## REFERENCES

1. K. Sumida, D. L. Rogow, J. A. Mason, T. M. McDonald, E. D. Bloch, Z. R. Herm, T. H. Bae and J. R. Long, *Chem. Rev.*, **112**, 724 (2012).
2. J. Wang, L. Huang, R. Yang, Z. Zhang, J. Wu, Y. Gao, Q. Wang, D. O. Hare and Z. Zhong, *Energy Environ. Sci.*, **7**, 3478 (2014).
3. Z. Yuan and M. R. Eden, *Ind. Eng. Chem. Res.*, **55**, 3383 (2016).
4. M. Aresta, A. Dibenedetto and A. Angelini, *Chem. Rev.*, **114**, 1709 (2013).
5. Z. Sumer and S. Keshin, *Ind. Eng. Chem. Res.*, **55**, 10404 (2016).
6. M. Mikkelsen, M. Jørgensen and F. C. Krebs, *Energy Environ. Sci.*, **3**, 43 (2010).
7. C. Maeda, Y. Miyazaki and T. Ema, *Catal. Sci. Technol.*, **4**, 1482 (2014).
8. J. Peng, H. J. Yang, Y. C. Geng, Z. D. Wei, L. H. Wang and C. Y. Guo, *J. CO$_2$ Util.*, **17**, 243 (2017).
9. V. Laserna, G. Fiorani, C. J. Whiteoak, E. Martin, E. Escudero-Adam and A. W. Kleij, *Angew. Chem. Int. Ed.*, **53**, 10416 (2014).
10. A. C. Kathalikkattil, R. Babu, R. Roshan, J. Tharun and D. W. Park, *Catal. Surv. Asia*, **19**, 223 (2015).
11. M. Liu, J. Lan, L. Liang, J. Sun and M. Arai, *J. Catal.*, **347**, 138 (2017).
12. J. Rintjema and A. W. Kleij, *ChemSusChem*, **10**, 1274 (2017).
13. J. W. Comerford, M. North and X. Wu, *Green Chem.*, **17**, 1966 (2015).
14. J. Liu, L. Chen, H. Cui, J. Zhang, L. Zhang and C. Y. Su, *Chem. Soc. Rev.*, **43**, 6011 (2014).
15. D. Farrusseng, S. Aguado and C. Pinel, *Angew. Chem. Int. Ed.*, **48**, 7502 (2009).
16. J. Y. Lee, O. K. Farha, J. Roberts, K. A. Scheidt, S. T. Nguyen and J. T. Hupp, *Chem. Soc. Rev.*, **38**, 1450 (2009).
17. A. Dhakshinamoorthy, A. M. Asiric and H. Garcia, *Chem. Soc. Rev.*, **44**, 1922 (2015).
18. J. Gascon, A. Corma, F. Kapteijn and F. X. Llabres i Xamena, *ACS Catal.*, **2**, 361 (2014).
19. J. H. Cavka, S. Jakobsen, U. Olsbye, N. Guillou, C. Lamberti, S. Bordiga and K. P. Lillerud, *J. Am. Chem. Soc.*, **130**, 13850 (2008).
20. S. E. Na, Y. R. Lee, S. H. Hong, M. S. Jang and W. S. Ahn, *Catal. Today*, **245**, 54 (2015).
21. L. Liu, J. Zhang, H. Fang, L. Chen and C. Y. Su, *Chem. Asian J.*, **11**, 2278 (2016).
22. J. Kim, S. N. Kim, H. G. Jang, G. Seo and W. S. Ahn, *Appl. Catal. A.*, **453**, 175 (2013).
23. V. Guillerm, F. Ragon, M. Dan-Hardi, T. Devic, M. Vishnuvarthan, B. Campo, A. Vimont, G. Clet, Q. Yang, G. Maurin, G. Frey, A. Vittadini, S. Gross and C. Serre, *Angew. Chem. Int. Ed.*, **10**, 9267 (2012).
24. T. Duren, F. Millange, G. Ferey, K. S. Walton and R. Q. Snurr, *J. Phys. Chem. C.*, **111**, 15350 (2007).
25. Y. S. Bae, A. O. Yazaydin and R. Q. Snurr, *Langmuir*, **26**, 5475 (2010).
26. D. W. Kim, R. Roshan, J. Tharun, A. C. Kathalikkattil and D. W. Park, *Korean J. Chem. Eng.*, **3**, 1973 (2013).
27. D. A. Yang, H. Y. Cho, J. Kim, S. T. Yang and W. S. Ahn, *Energy Environ. Sci.*, **5**, 6465 (2012).
28. O. Zalomaeva, A. M. Chibiryaev, K. A. Kovalenko, O. A. Kholdeeva, B. S. Balzhinimaev and V. P. Fedin, *J. Catal.*, **298**, 179 (2013).
29. M. H. Beyzavi, C. J. Stephenson, Y. Liu, O. Karagiaridi, J. T. Hupp and O. K. Farha, *Frontiers Energy Res.*, **2**, 1 (2015).
30. K. R. Roshith, J. Tharun, R. Babu, G. Y. Hwang, A. C. Kathalikkattil, D. W. Kim and D. W. Park, *Appl. Catal. B. Env.*, **182**, 562 (2016).
31. L. Han, H. J. Choi, S. J. Choi, B. Liu and D. W. Park, *Green Chem.*, **13**, 1023 (2011).
32. K. R. Roshith, G. Mathai, J. Kim, J. Tharun, G. A. Park and D. W. Park, *Green Chem.*, **14**, 2933 (2012).
33. R. Babu, A. C. Kathalikkattil, R. Roshan, J. Tharun, D. W. Kim and D. W. Park, *Green Chem.*, **18**, 232 (2016).
34. A. C. Kathalikkattil, R. Babu, R. Roshan, J. Tharun, H. Lee, H. Kim, E. Suresh and D. W. Park, *J. Mater. Chem. A.*, **3**, 22636 (2015).
35. J. Tharun, G. Mathai, A. C. Kathalikkattil, R. Roshan, Y. S. Won, S. J. Cho, J. S. Chang and D. W. Park, *ChemPlusChem*, **80**, 715 (2015).
36. J. Tharun, K. M. Bhin, R. Roshan, D. W. Kim, A. C. Kathalikkattil, R. Babu, H. Y. Ahn, Y. S. Woo and D. W. Park, *Green Chem.*, **18**, 2479 (2016).
37. R. Babu, R. Roshan, Y. Kim, Y. H. Jang, J. F. Kurisingal, D. W. Kim and D. W. Park, *J. Mater. Chem. A.*, **5**, 15961 (2017).
38. A. C. Kathalikkattil, D. W. Kim, J. Tharun, H. G. Soek, R. Roshan and D. W. Park, *Green Chem.*, **16**, 1607 (2014).
39. T. Ema, Y. Miyazaki, J. Shimonishi, C. Maeda and J. Hasegawa, *JACS*, **136**, 15270 (2014).
40. H. S. Ryu, R. Roshan, M. I. Kim, D. W. Kim, M. Selvaraj and D. W. Park, *Korean J. Chem. Eng.*, **34**, 428 (2017).
41. M. North, R. Pasquale and C. Young, *Green Chem.*, **12**, 1514 (2010).

# Supporting Information

# Zirconium-based isoreticular metal-organic frameworks for $CO_2$ fixation via cyclic carbonate synthesis

**Hye-Min Jeong, Roshith Roshan, Robin Babu, Hyeon-Jun Kim, and Dae-Won Park[†]**

Division of Chemical and Biomolecular Engineering, Pusan National University, Busan 46241, Korea
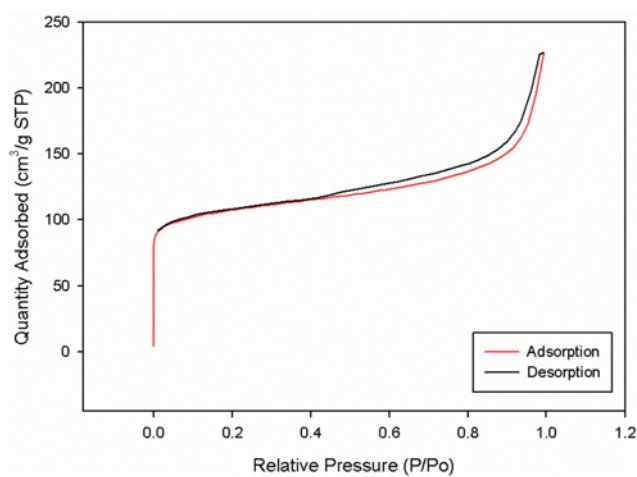
**Fig. S1.** $N_2$-adsorption and desorption of MIL-140A.
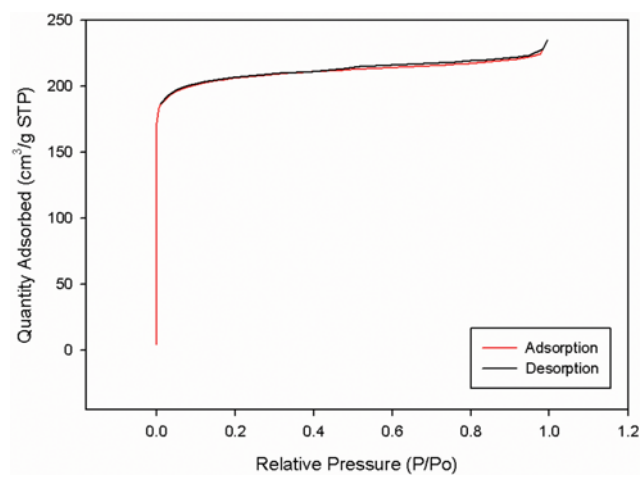


**Fig. S2.** $N_2$-adsorption and desorption of MIL-140C.
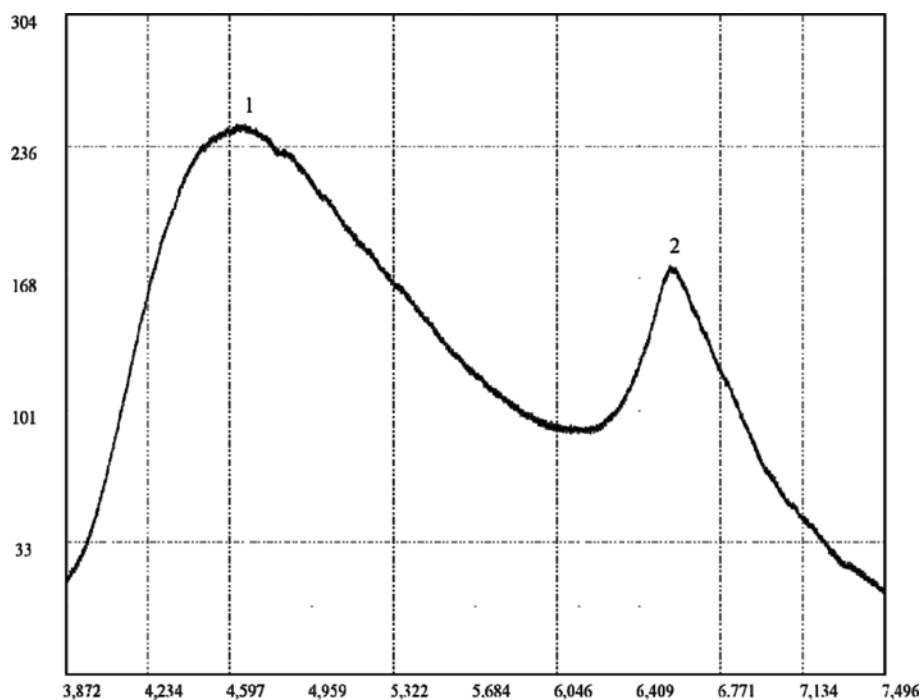


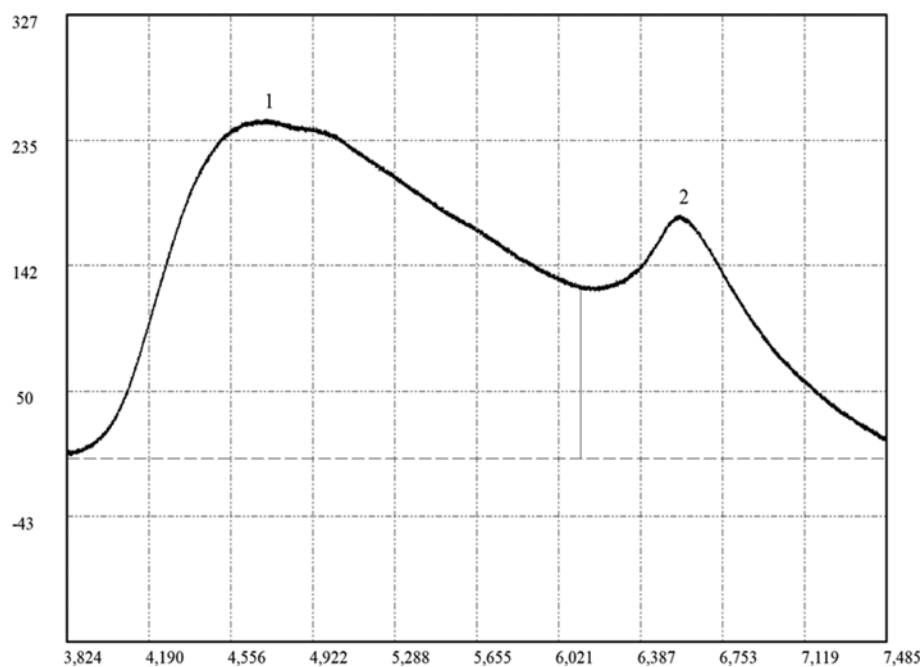**Fig. S3.** $CO_2$ TPD of MIL-140A.

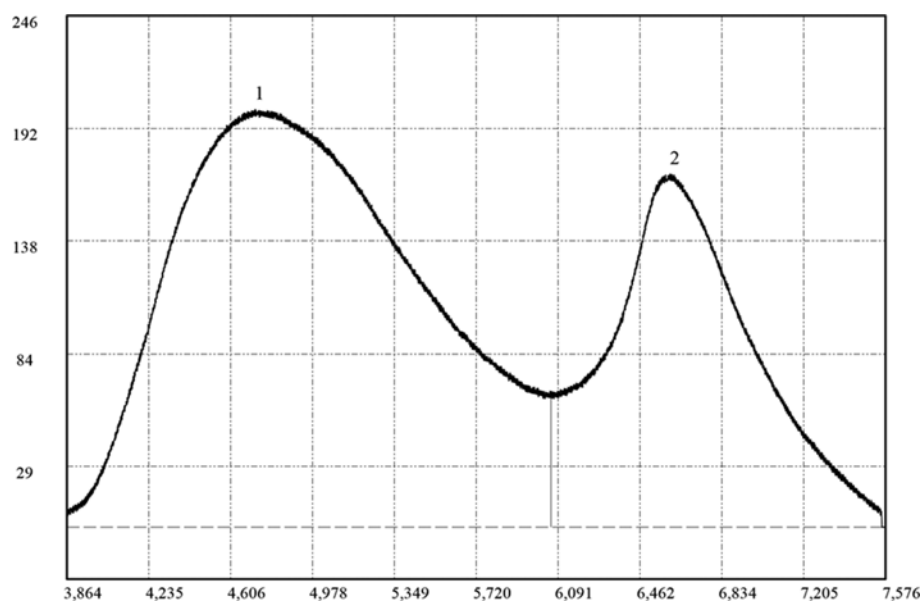**Fig. S4. NH$_3$ TPD of MIL-140A.**
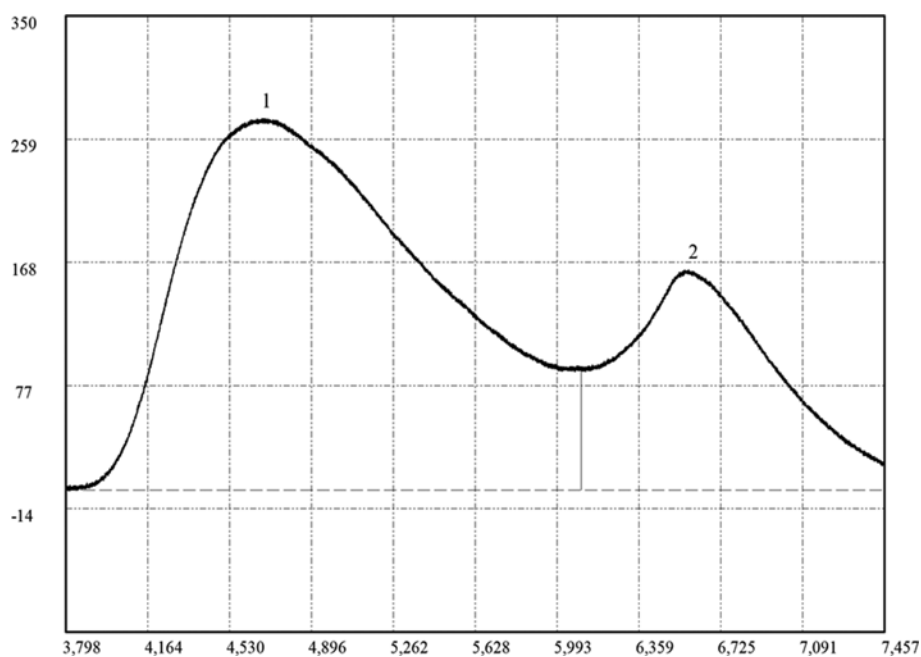


**Fig. S5. CO$_2$ TPD of MIL-140C.**

**Fig. S6. NH₃ TPD of MIL-140C.**

**Table S1. Elemental analysis of MIL-140A and MIL-140C**

MIL-140A

| Element | Experimental (%) | Theoretical (%) |
|---------|------------------|-----------------|
| C | 35.32 | 35.4 |
| H | 2.52 | 1.47 |
| O | 27.94 | 29.5 |

MIL-140C

| Element | Experimental (%) | Theoretical (%) |
|---------|------------------|-----------------|
| C | 43.83 | 48.40 |
| H | 2.51 | 2.32 |
| O | 21.97 | 22.52 |

**Table S2. ICP of MIL-140A and MIL-140C**

MIL-140A

| Element | Experimental (%) | Theoretical (%) |
|---------|------------------|-----------------|
| Zr | 32.14 | 33.63 |

MIL-140C

| Element | Experimental (%) | Theoretical (%) |
|---------|------------------|-----------------|
| Zr | 22.44 | 26.26 |